Journal of Nuclear Materials 398 (2010) 35–42

Contents lists available at ScienceDirect

Journal of Nuclear Materials

journal homepage: www.elsevier.com/locate/jnucmat

3 MW solid rotating target design

T. McManamy [a,*], M. Rennich [b], F. Gallmeier [b], P. Ferguson [b], J. Janney [b]

[a] Oak Ridge National Laboratory, P.O. Box 2008 MS6473, Oak Ridge, TN 37831-6473, USA
[b] Oak Ridge National Laboratory, Oak Ridge, TN, USA

A B S T R A C T

A rotating solid target design concept is being developed for potential use at the second SNS target station (STS). A long pulse beam (~1 ms) at 1.3 GeV and 20 Hz is planned with power levels at or above 1 MW. Since the long pulse may give future opportunities for higher power, this study is looking at 3 MW to compare the performance of a solid rotating target to a mercury target. Unlike the case for stationary solid targets at such powers this study indicates that a rotating solid target, when used with large coupled hydrogen moderators, has neutronic performance equal to or better than that with a mercury target, and the solid target has a greatly increased lifetime. Design studies have investigated water cooled tungsten targets with tantalum cladding approximately 1.2 m in diameter, and 70 mm thick. Operating temperatures are low (<150 °C) with mid-plane, top and bottom surface cooling. In case of cooling system failure, the diameter gives enough surface area to remove the decay heat by radiation to the surrounding reflector assemblies while keeping the peak temperatures below approximately 700 °C. This temperature should mitigate potential loss of coolant accidents and subsequent steam, tungsten interaction which has a threshold of approximately 800 °C. Design layouts for the sealing systems and potential target station concepts have been developed.

1. Introduction

A design concept for a rotating solid target that could be used at up to 3 MW for a second target station at SNS has been developed. A one year design study was completed to develop the conceptual design of the target, to show how it could be incorporated into an optimized target station arrangement, maintained remotely and to develop the design of the drive, seals and bearing to a level where testing of these elements could be done the following year. The overall intent has been to develop the rotating solid target design concept to a level where it would be a realistic alternative to a liquid mercury target for a high power target. The potential advantages include much longer target lifetimes, equivalent or better neutronic performance and significantly reduced remote handling requirements if water is the primary coolant. Three megawatt was chosen because it is probably an upper bound for the power that could be delivered to the second SNS target station. Recent rotating target studies have shown promising results for lower power levels [1,2]. For this study we have chosen to look at tantalum clad tungsten with water cooling. Good operating and fabrication experience with these materials has been shown at the ISIS first and second target stations and at the KENS facility.

2. Design requirements and preliminary configuration selection

The second target station (STS) at SNS is to be optimized to produce the brightest cold neutron beams from large para-hydrogen moderators with a 1.3 GeV proton beam at 20 Hz. The initial power level is expected to be on the order of 1 MW with the possibility of up to 3 MW in the future. For high power operation approximately 1 ms pulses will come directly from the linac. The design must support 18–24 beamlines viewing the moderators positioned above and below the target. The target, moderator and reflector systems must be remotely maintained. Decay heat loads and heat removal systems for the target under off normal conditions must be developed in conjunction with the facility safety assessment.

Preliminary evaluations indicated that a target diameter of 1–1.5 m would give lifetimes on the order of 5–8 years for 10 dpa on the window at 3 MW with low average heat loads. A diameter of 1.2 m was selected for this study based on preliminary thermal analysis of removing the decay heat with a cooling system failure by conduction in air and thermal radiation to the surrounding reflector assemblies while maintaining the tungsten below approximately 700 °C. This temperature should prevent vaporization of the tungsten with steam. A tungsten target region 70 mm to 80 mm was selected to be compatible with the same vertical size beam as at SNS with some allowance for an off-center beam. The tungsten would be contained within a stainless steel shell. Rotation at 30–60 rpm will avoid pulses overlapping. Two beam

* Corresponding author.
E-mail address: mcmanamytj@ornl.gov (T. McManamy).

0022-3115/$ - see front matter © 2009 Elsevier B.V. All rights reserved.
doi:10.1016/j.jnucmat.2009.10.007

profiles were investigated. One was a double Gaussian with a 15 mm vertical sigma and a 45 mm horizontal sigma. This is a realistic beam profile that could be obtained by expanding the linac beam. Another profile considered was flat over a 60 mm vertical by 180 mm horizontal region. To obtain this a small beam spot would be rastered during the 1 ms pulse in the rectangular region, similar to what has been proposed for the Material Test Station at Los Alamos National Laboratory [3]. At 1.3 GeV the peak current density for the Gaussian distribution is .544 A/m^2 and 0.214 A/m^2 for the flat profile.

3. Neutronics design

The neutronics design task is twofold. Firstly, it is instrumental to find a target–reflector–moderator assembly (TMRA) that provides the best neutron output into beamlines. Secondly, neutronics data are needed to answer various engineering questions, like energy deposition data for subsequent thermal and structural analyses, the heat input of the moderator units for designing the cryogenic system, and material damage for component lifetime predictions. Ultimately both tasks are interwoven, since engineering establishes constraints that are folded back into further optimization studies.

All multi-particle transport analyses were performed with MCNPX_2.5.0 [4]. Global optimizer strategies applying Bayesian algorithms were applies for the neutron performance optimization of the TMRA [5].

3.1. TMRA optimizations

About two years ago, extensive studies were performed for a second SNS target station optimized for high-intensity cold neutron fluxes [6]. Numerous analyses were performed investigating potential liquid target materials, reflector and moderator options, and moderators in wing, slab and flux-trap configurations. Each considered TMRA configuration was parameterized and analyzed for the optimum parameter set applying global optimization strategies. As optimization parameters basic quantities such as moderator dimensions, pre-moderator thickness and moderator position with respect to the target were used. Details of the optimization procedure and the analyses will be reported elsewhere [7].

A TMRA configuration of two large volume cylindrical para-hydrogen moderators positioned on top and bottom of a flat target in wing configuration and surrounded by a layer of ambient light water and by a beryllium reflector emerged as the optimum solution considering the 18–24 beam ports the moderators have to serve. Beam lines view the cold source at three ports at viewing areas of 100 mm width and 120 mm height.

The resulting optimum TMRA configuration was used as baseline substituting the liquid mercury target by a rotating target. Tantalum clad tungsten was considered as first choice target material for its high atomic mass and high density, but also for the experience base as target material at existing spallation neutron sources such as ISIS, LANCE and IPNS. Scoping studies of energy deposition and heat removal lead to a design with a bulk tungsten ring of 600 mm outer and 350 mm inner radius backed on the inside by a stainless steel hub. Initially it was assumed that the bulk tungsten could be edge-cooled by forced water flow on the top and bottom surfaces and across the front face. Later a central 1.5 mm cooling water channel was added to improve cooling and reduce thermal stresses. A small step was included in the central channel to avoid streaming of high-energy protons to the central steel hub. Fig. 1 shows the layout of the final optimized TMRA with a para-hydrogen moderator height and diameter of 120 mm and 220 mm, respectively, pre-moderator thicknesses of 13 mm, 7 mm and 7 mm, at the bottom, top and radially, respectively, with a target height of 70 mm and a 5 mm step-up of the central cooling channel at 525 mm radius. The optimal moderator axis position arrived at 489 mm distance from the rotating target axis. In this configuration the cold flux of energies below 5 meV in beam line at 10 meter distance viewing a 100×120 mm^2 area of moderator is about 5.7×10^{-8} n/cm^2/proton and equivalent to that of a TMRA driven by a mercury target. The gain of the neutron production

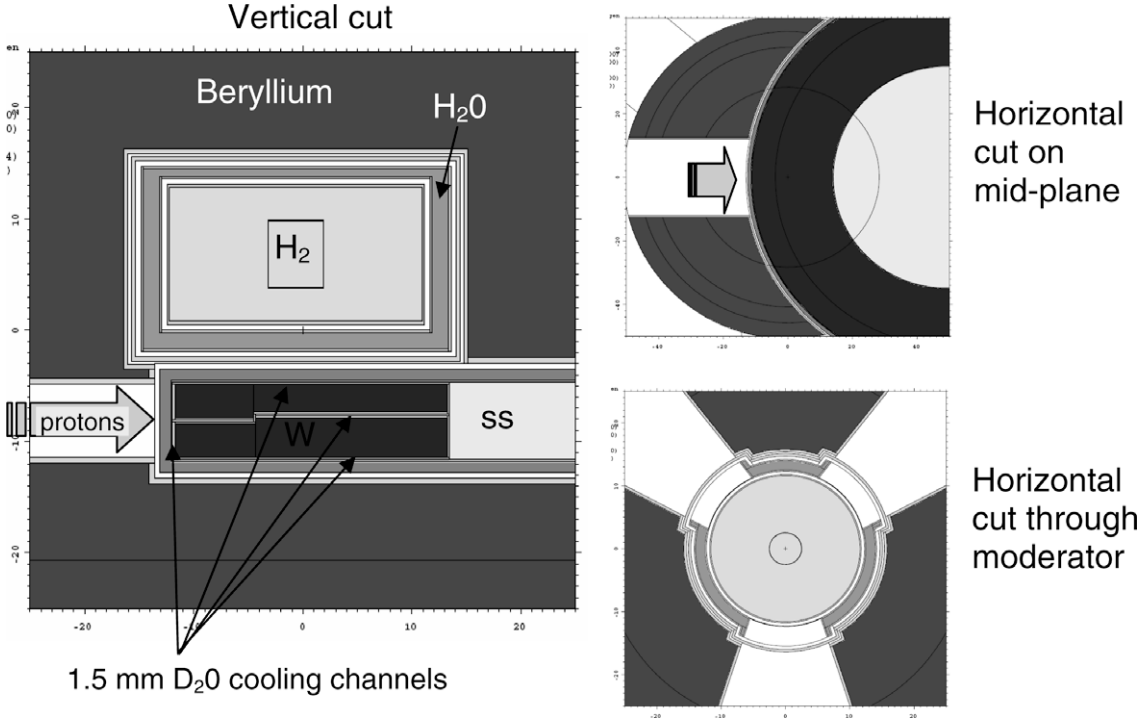

Fig. 1. Target, moderator, reflector assembly (TMRA) of a second SNS target station based on a rotating target.

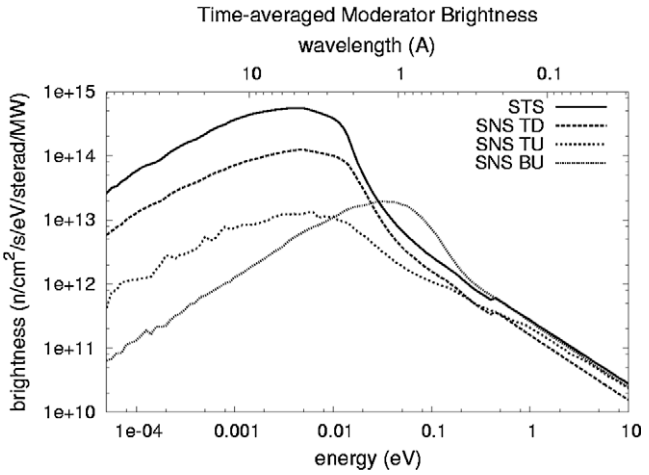

Fig. 2. Neutron brightness of second SNS target station (STS) compared to performance of the top upstream (TU) and top downstream (TD) supercritical hydrogen moderators and the bottom upstream (BU) ambient water moderator of the present SNS target station (SNS).

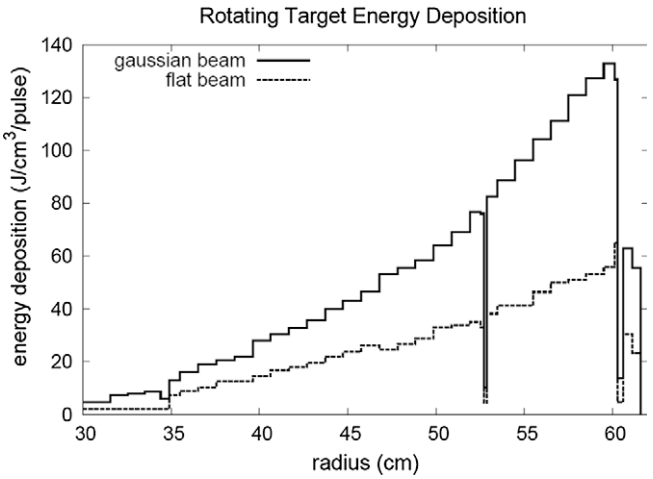

Fig. 3. Energy deposition rates in rotating target in beam centerline: cases for Gaussian and flat beam profile are compared. The dip at 53 cm radius is caused by the step up of the central cooling channel.

Table 1
Estimated dpa values in STS key components based on 3 MW power.

Component	Gaussian beam (dpa/year)	Flat beam (dpa/year)
Target vessel (SS316)	1.95	1.6
Tantalum cladding	2.7	1.8
Tungsten bulk	3.1	2.2
Moderator structure (Al6061)	21	18

in target material is about equalized by the losses of neutron absorptions in the less effective target configuration. It is noteworthy that the penalty in cold neutron flux due to a central cooling channel is as low as 3%. The flat proton beam profile provides a gain of 2% in neutron performance compared to the Gaussian profile beam. A comparison of time-averaged neutron brightness of the STS moderator against the moderators at the present SNS target station (SNS) is shown in Fig. 2, illustrating that STS will give a factor of 5 higher cold neutron brightness. From the factor of 5 gain in brightness, an approximate factor of two is gained by positioning the STS in the optimum target position while the coupled moderators at the present SNS target station are located in the less favorable downstream positions [10].

3.2. Radiation-induced material damage

For the optimized configuration, the material damage of key components was assessed folding dpa cross sections [8] with neutron and proton fluxes as listed in Table 1. While the rotating target structures spend only a fraction of the operations time in the high flux zone, the moderator structures are exposed permanently to severe radiation fields. Hence it is not surprising that the moderator structures exhibit about a factor of 10 higher dpa rates resulting in shorter life times and higher frequency of exchange than the rotating target structure. For a 10 dpa limit on the steel target vessel the lifetime would be 5–6 years while the moderators would likely need to be replaced about once a year.

Radiation-induced energy deposition in the target and moderator assemblies was assessed for the optimized TMRA as a basis for subsequent thermal and structural analyses and for estimating the cooling capacity of the moderator cryogenic systems.

From 3 MW incident beam power, 1.9 MW is deposited into the target structure, 10.8 kW into the cryogenic moderator part,

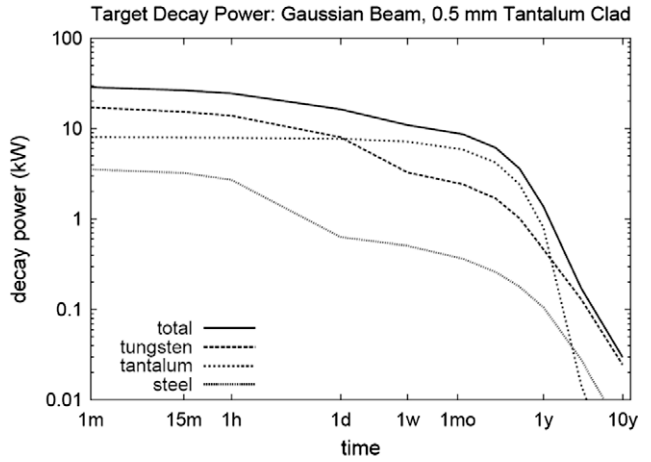

Fig. 4. Integral decay power of rotating target components irradiated at 3 MW for 10 years.

6.3 kW into the moderator's pre-moderator system. The local energy deposition in the target structure reaches 125 J/cc/pulse in the bulk tungsten for the Gaussian profile beam, and drops to half the value for the flat profile beam as shown in Fig. 3. For the Gaussian beam profile with the target rotating at approximately 30 rpm the peak time average heating is approximately 110 W/cc versus the 2.5 kW/cc heating if the target was stationary.

The target was subdivided into a three-dimensional cylindrical mesh for obtaining energy deposition profile data sets per proton pulse that were with minimal editing handed off to ANSYS thermal and structural analyses.

The decay power of the target structure was determined assuming 10 years operation at 3 MW power feeding MCNPX calculated neutron flux and isotope production rates into the nuclear inventory analyses using the CINDER90 code applying the activation script tool [9]. The timeline of the resulting decay is shown in Fig. 4 for tungsten blocks clad by a 0.5-mm-thick tantalum. A significant quantity of decay power is observed in the tantalum cladding, which dominates the total decay power one day after shutdown. The problem is even more severe with increased thickness of the tantalum cladding increasing the total decay power from 32 kW for 0.5 mm cladding to 44 kW at 2 mm as shown in Fig. 5. Generally, in a tungsten/tantalum target assembly the de-

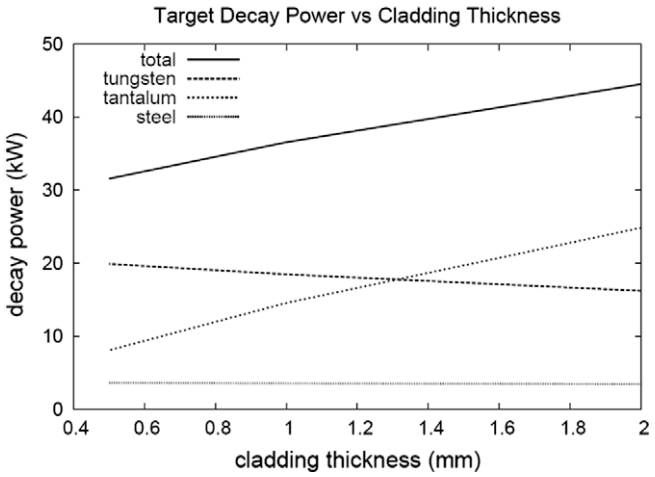

Fig. 5. Variation of decay power immediately after shutdown with tantalum cladding thickness.

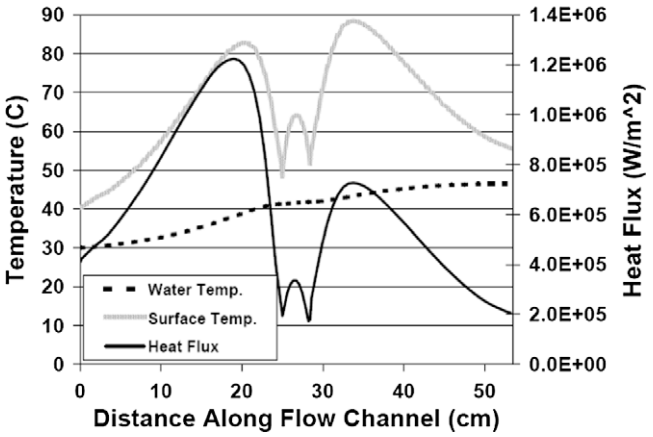

Fig. 7. Thermal hydraulic conditions for 60 rpm rotation, flat beam profile, just after beam pulse. Distance of 0–25 cm is in center channel starting at 35 cm radius, 25–28.5 cm is outside face, and 28.5–53.5 cm is top and bottom cooling channel.

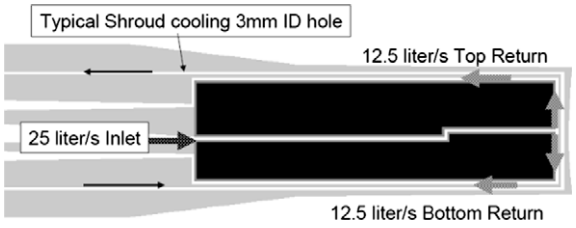

Fig. 6. Target water cooling flow with 1.5 mm high radial inlet flow channel on the mid-plane and split return 1.5 mm channels on the front, top and bottom surfaces.

cay power is governed by isotopes generated by thermal neutron absorption reactions at the target/moderator and target/reflector interfaces rather than by spallation reactions, creating peaking in the local decay energy deposition rates close at the cooling channels. Other solid target decay heat results can be found in reference [11].

4. Target module design

Preliminary 2D thermal analysis for steady state operation and decay heat removal of 36 kW under off normal conditions established the basic size for the target module. A 1.2 m diameter was found to keep the tungsten below approximately 700 °C by conduction through air and thermal radiation to the surrounding reflector assemblies. This was based on a 5 mm gap between the reflector assemblies at 50 °C and the target and with enhanced emissivity of 0.8 for the reflector and target shell. With helium in all gaps the temperatures would be on the order of 400 °C. Loss of primary coolant flow was considered an expected event and cooling within the shroud was included to prevent boiling of stagnant primary coolant.

The ANSYS finite element software package was used to analyze the thermal response and resulting stresses in the target considering the heat transfer mechanisms of body heat generation from proton and neutron irradiation, convection to the cooling water, and conduction within the segments. The initial analyses were based on water cooled, free-standing, unconstrained tantalum clad tungsten segments. Next, various mechanical constraints were added to develop a configuration which maintains stresses at an acceptable level inside the stainless steel shroud. Finally, a detailed design of the stainless steel shroud was created to minimize stresses from thermal expansion of the steel and containment of the tungsten and coolant while providing flow paths for coolant and minimizing material in the beam path and between the tungsten and the moderator assembly.

The cooling systems considered for the solid rotating target were required to be both simple and robust. Two configurations were considered, one featured cooling on the top, bottom and outer face of the segments while the other featured a horizontally split segment with cooling in the center channel as well as the top, bottom, and outer face as shown in Fig. 6. Both configurations assumed a flow rate of 25 l/s with 1.5 mm high coolant passages. These gave heat transfer coefficients of approximately 2×10^4 W/m^2/K at the outside radius at a flow velocity of 4.4 m/s and a bulk coolant temperature rise below 20 °C assuming 70% of beam power is thermally absorbed in the tungsten. The center cooled configuration produced significantly lower temperatures and resulting stresses, with maximum temperature of 127 °C compared to 298 °C and maximum 1st principle stress of 101 MPa versus 295 MPa. The center cooling channel maintained a substantially lower peak temperature due to a shorter conduction path to the cooling channels as well as having a cooling channel in the region of highest heat deposition. The stress level seen in the configuration without central cooling could potentially cause failure of the clad or fracture of the tungsten segment, due to tungsten's low ductility in tension, especially as radiation damage accumulates, although limited fatigue data for irradiated tungsten subjected to thermal stress cycles is available. Therefore, only the center cooled target configuration was considered for further analysis.

After determining a potential cooling configuration, the system for containing the segments during rotation had to be developed. Transient beam pulsing, at a rate of 20 Hz and pulse length of 1 ms, was applied to a 3D model of one of the 20 tantalum clad tungsten segments by directly applying single pulse heat deposition data from neutronics analysis of a Gaussian beam profile. Cooling flow was simulated using convection coefficients from the Dittus–Boelter correlation [12] and an inlet temperature of 30 °C. A plot of the water temperature, as well as the surface temperature and heat flux, is shown in Fig. 7, showing the outlet temperature to be 47 °C just after the pulse had passed the segment.

As a baseline, a segment with no restrictions to expansion was simulated and showed maximum temperature of 171 °C and 1st principal stress in the tungsten of 84 MPa. Maximum stresses were lower in the 3D simulations than the previous 2D simulations due to segmentation of the tungsten, which provides less restriction to expansion than a solid tungsten ring. Several configurations involving bonding of the tungsten segments to a stainless steel

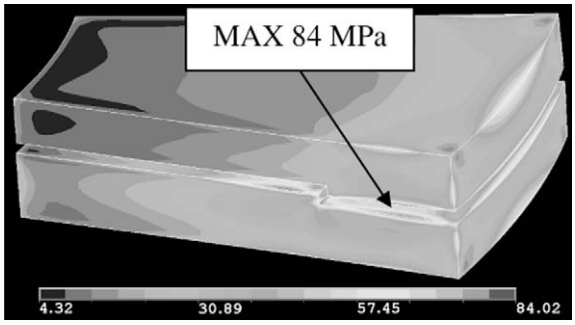

Fig. 8. First principle stresses (MPa) in tungsten segment just after Gaussian beam pulse for 30 rpm rotation rate with free spacer and spring constraint. Shroud, spacers, springs, and cladding are removed for clarity.

Table 2
Maximum temperatures and stresses for tungsten (1st Prin.) and tantalum cladding (Von Mises) for mechanical restraint with springs and spacers.

Beam profile	Rotation rate (rpm)	Maximum temperature (°C)	Pre-pulse maximum stress (MPa)		Post-pulse maximum stress (MPa)	
			Ta	W	Ta	W
Gaussian	30	171	59	66	83	84
Flat	30	168	55	67	70	90
Flat	60	151	68	71	66	79

hub were considered; however, all revealed maximum first principal stress levels on the order of 400 MPa and shear stress levels at the interface which suggested that debonding was likely to occur. Any system which involved bonding stainless steel to the tantalum clad produced unacceptable stress levels due to the large difference in thermal expansion coefficients. Next, systems involving spacers and springs to allow thermal expansion of the segments were considered. Twelve total tantalum spacers, 4 in each location were placed between the top and bottom bricks, between the bottom brick and the shroud, and between the outer radius of the bricks and the outer radius of the shroud in addition to 4 springs between the top of the segment and the shroud and 2 springs at the inner radius. Contact algorithms were used to simulate the spacers with no bond to the shroud, revealing a stress state in the tungsten identical to the initial free expansion simulation, as seen in Fig. 8.

Additionally, the maximum Von Mises stress in the tantalum was reduced to 83 MPa and the maximum shear stress at the tungsten–tantalum interface was 14 MPa. Results from the study of mechanical restraint for both the Gaussian and rastered flat beam profile can be found in Table 2. For every beam profile and rotation rate, the free spacer and spring system resulted in stresses identical to the unrestrained models.

Initial shroud modeling was performed by utilizing different simple shroud designs during the study of mechanical constraint systems. The shrouds examined were constructed with either 7 or 10 mm thick 316 stainless steel walls. Contact modeling was used to transfer forces from the tungsten segments to the shroud, but coolant pressure was neglected. Thermal stresses near the cooling holes in the beam path were as high as 250 MPa in the case of the 10 mm shroud with the Gaussian beam profile, but as low as 140 MPa for the 7 mm shroud with the flat beam profile at 60 rpm. Furthermore, simple axisymmetric modeling of 0.3 MPa internal coolant pressure shows extreme stress levels at the meeting with the hub for both wall thicknesses, and additionally at the outer corners for the 7 mm wall, indicating that a complex shape was required to fulfill the shroud requirements. The final optimized

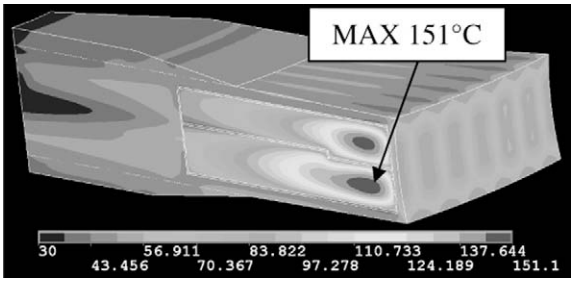

Fig. 9. Temperature profile (°C) just after flat beam pulse for 60 rpm rotation rate with optimized shroud.

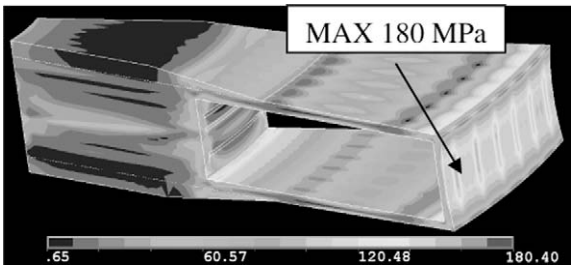

Fig. 10. Von Mises stresses (MPa) in 316 Stainless Steel shroud just after flat beam pulse for 60 rpm rotation rate with .3 MPa internal pressure and simulated tungsten gravity and inertia loads.

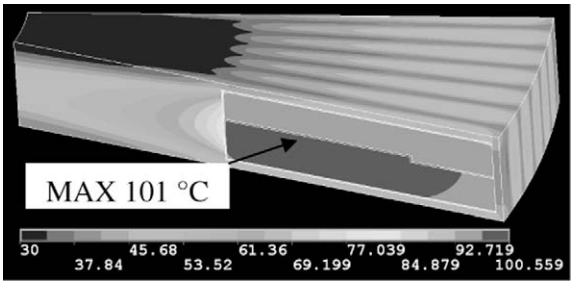

Fig. 11. Temperature profile (°C) resulting from loss of primary cooling, but retention of secondary cooling, for decay heat for a tungsten target with 1 mm tantalum cladding.

Table 3
Maximum temperatures and Von Mises stresses for optimized stainless steel shroud.

Beam profile	Rotation rate (rpm)	Maximum temperature (°C)	Pre-pulse maximum stress (MPa)	Post-pulse maximum stress (MPa)
Gaussian	30	115	215	290
Flat	30	95	165	201
Flat	60	92	166	180

shape consisted of a concave wall with 7 mm minimum thickness in the beam path while the horizontal walls tapered from 18 mm at the hub to 9 mm at the outer corner. Maximum temperatures in the shroud were limited to 115 °C in the shroud and 151 °C in the segments, as seen in Fig. 9.

Internal coolant pressure was included in the final optimization modeling, resulting in peak Von Mises stress levels in the shroud nose of 180 MPa in the case of flat beam at 60 rpm, as seen in Fig. 10. It should be noted that square holes were used to represent

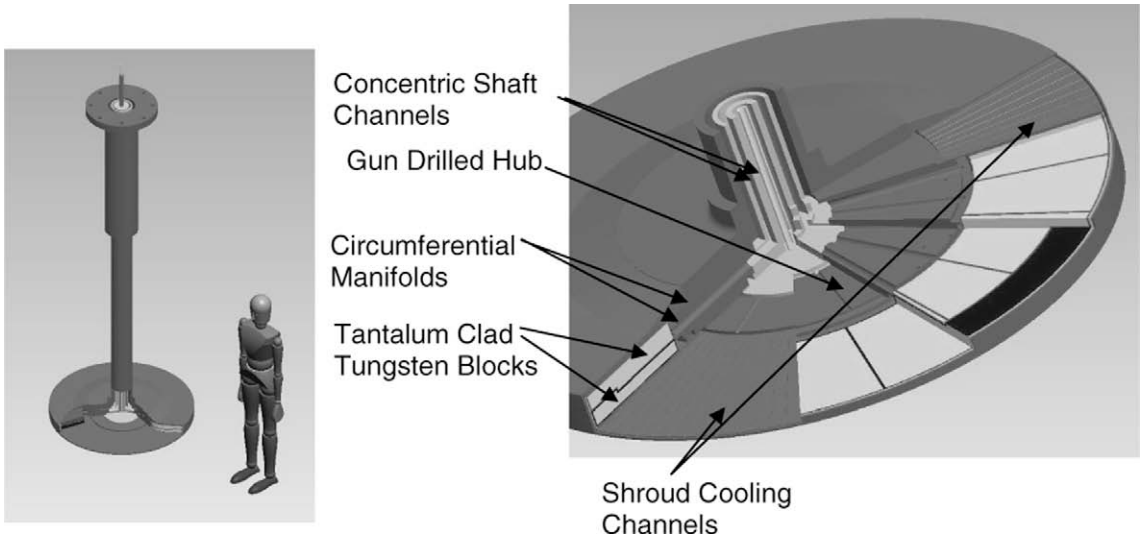

Fig. 12. Rotating target module.

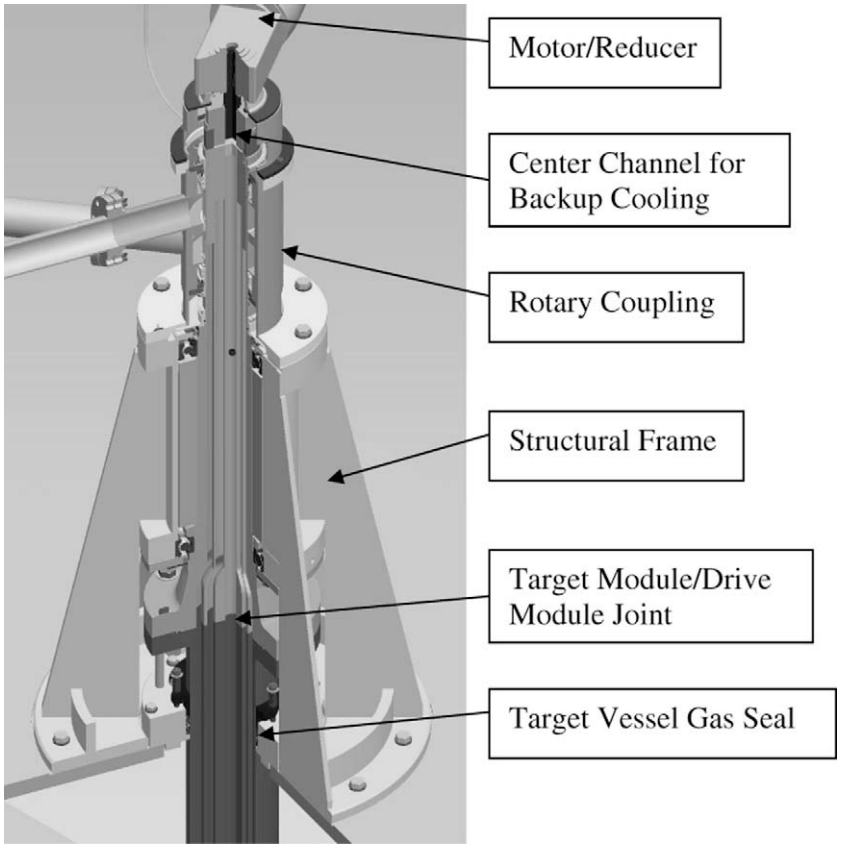

Fig. 13. Drive module.

the secondary cooling flow channels, resulting in high stresses at geometric discontinuities. The 3 mm diameter secondary cooling channels shown in Fig. 6 were included at a spacing 3° in order to keep primary coolant from boiling due to decay heat in case of a loss of primary cooling system flow as shown in Fig. 11. Table 3 summarizes the maximum stress levels in the optimized shroud for other beam profiles, and reveals all cases are acceptable by the ASME BPVC thermal stress limit of 345 MPa for 316 stainless steel.

5. Mechanical configuration

The mechanical configuration of STS rotating target was developed in conjunction with the neutronic and thermal/stress studies. At the most basic level the orientation of the target disk about the vertical axis established the drive system, moderator and neutron beam interfaces. Internal routing of the 25 l/s cooling water flow through the target axle determined the minimum shaft diameter at 175 mm. It also necessitated a large, two-channel rotary

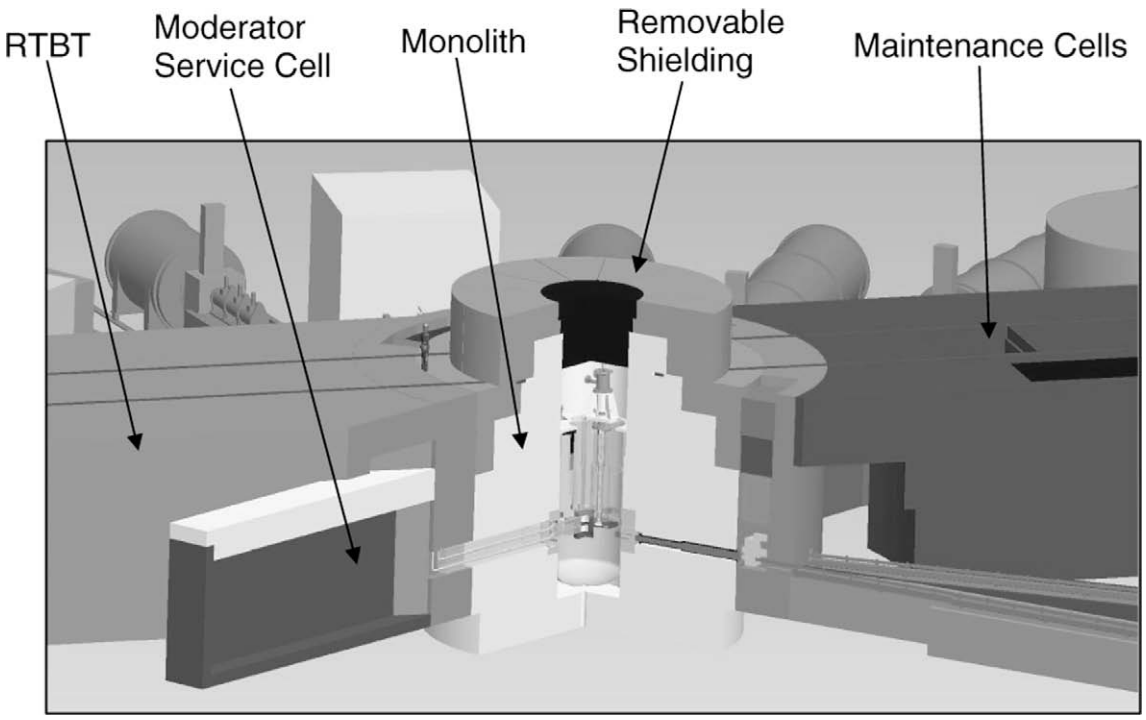

Fig. 14. SNS target station two configuration for a rotating target.

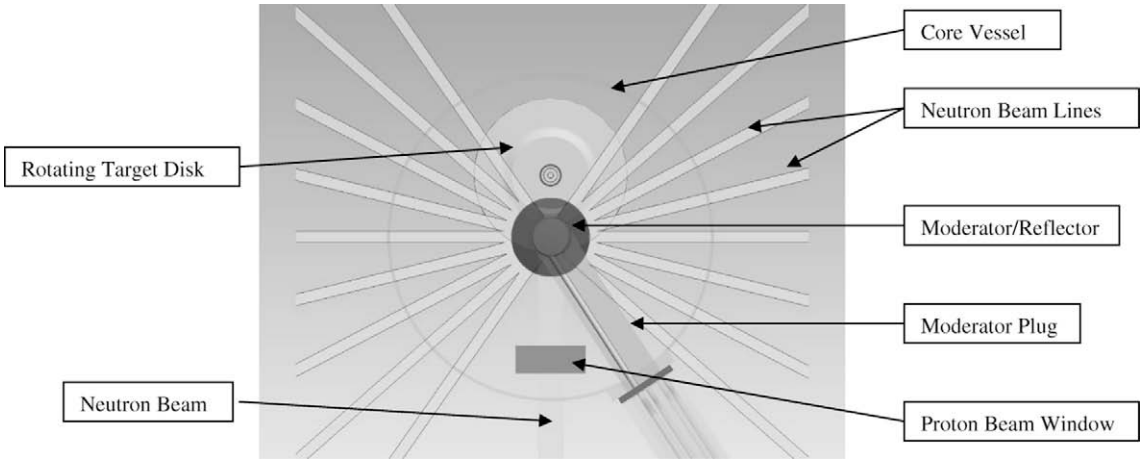

Fig. 15. Plan view of core target system components.

coupling to accommodate the cooling water interface with the pumping system. Containment of the heavy water coolant placed a premium on superior sealing and spilled water monitoring and capture in the event of both large and small leaks. Backup shroud cooling (1.2 l/s) requirements added the requirement for independent flow channels down the center of the axle and a second rotary coupling. Finally, given the different operational life-times for the target (5–8 years), moderators (1–2 years) and proton beam window the basic layout of the target system needs to allow for individual handling and maintenance of these components.

The rotating target assembly logically divides into two major subassemblies; the highly activated target disk and a grouping of the subassemblies required to operate the target disk; the drive, primary water seals, backup cooling water coupling and a frame to hold and align the target assembly as shown in Figs. 12 and 13. A study of the full range of practical assembly and maintenance handling options led to a long vertical plug mounted target assembly. Mounting the support subassemblies outside the target vessel approximately 3.5 m above the target disk reduces the radiation exposure to that emitted by the cooling water exiting the target and passing through the axle and rotary coupling. At the computed 100 rads/h this remote position will allow for the use of commercially available components and relatively efficient maintenance access. These critical advantages are somewhat off-set however; by the need for a dynamic gas seal at the axle pass-thru in the vessel lid, and the need for precision alignment between the drive module at the top of the target assembly and the moderators at the bottom.

Packaging the target assembly drive and sealing components into a single modular subassembly fits the design goals of precision alignment, efficient maintenance, and practical off-line preoperational functional checks. The proposed modular configuration is shown in Fig. 13. The arrangement packages the key subassemblies along the axle starting with the vessel gas seal at the bottom. In

addition to the sealing the vessel for rough vacuum and operation with helium at approximately 0.1 MPa, the seal must be maintainable in-place. The current concept is based on a four-ring graphite packing seal with an intermediate helium gas injection capability to prevent air leakage into the vessel. The 0.5 m diameter flanged drive module to target module flange connection is located above the vessel gas seal. Adequate space is provided for gas seal maintenance and joint assembly and disassembly on either side of the flange. Above the module coupling flange is the axle bearing assembly which is designed to cantilever support the target module. Two deep groove roller bearings, mounted 0.66 m apart, are used to achieve precision assembly and running tolerances. Stability is achieved by mounting the bearing assembly in a rigid frame designed to minimize deflections and vibrations. The cooling water rotary coupling is mounted to the top of the bearing frame. It incorporates two welded metal bellows style graphite face seals designed for long life operation. An intermediate seal between the 4" schedule 40 feed and discharge lines is a close tolerance non-contact gap seal which will allow a small amount of bypass flow but will not require maintenance. A conventional variable speed motor/reducer drive is mounted to the top of the water coupling. As with the vessel gas seal it will be packaged to permit in-place maintenance and replacement. Finally, at the top of the drive provisions are made to insert the backup cooling tubes through the center of the axle. The two tubes will be sealed at the top of the axle and connected to the independent water supply system via a conventional rotary coupling. The complete backup cooling water assembly can be maintained or replaced in situ.

6. Target station configuration

A rotating target based SNS–STS is shown in Fig. 14. A key feature of the proposed target system is a 2.5 m diameter core vessel designed to contain the target and all actively cooled shielding. With the center of the 1.2 m diameter rotating target positioned downstream from the moderators it is possible to install the proton beam window inside the vessel as shown in Fig. 15. This position simplifies the proton beam window assembly since it requires a vacuum seal only on the proton beam tube side. The vertical plug mounted assembly also fits nicely into the overall target station maintenance scheme. Inclusion of a stepping function designed to expose discrete areas of the window to the beam for limited times without changing the entire assembly is also proposed to improve the reliability of the overall facility.

Mounting the moderators into a horizontal, rail mounted plug was found to be the most effective assembly option. This arrangement allows for independent change-out and maintenance of the moderators; an important requirement given the expected difference in life. This will require an independent special purpose hot cell located on the upstream side of the instrument floor. The hot cell could block at least one of the instrument slots; however, this loss may be off-set by shifting the beam line array downstream.

The target plug will require a large, shielded handling container for removal and transport to maintenance and storage cells. Given the size of this assembly (>100 tons when loaded) and the cost of a large overhead bridge crane, a rail system is proposed for the STS high bay. This arrangement logically arranges maintenance and handling activities along the centerline of the high bay which will optimally locate the maintenance cells away from the instruments and allow for manipulator access from two or more sides of the cells. The shielded transport container will also be used to move activated proton beam window modules to the maintenance cells for size reduction and packaging.

7. Conclusion

A rotating solid target design at 3 MW has been shown to give equal or better neutronic performance than a liquid metal target with the advantage of a much longer target lifetime. The use of water cooling will also avoid added complexities associated with highly activated liquid metal targets. High decay heat is one potential drawback, but design solutions for heat removal are possible. Further safety studies and fabrication studies for the tungsten wedges are planned.

Acknowledgments

The authors would like to thank Dr. Günter Bauer for many helpful comments during this study and also for his early contributions to the rotating target concept. Dr. R. Kent Crawford also helped to define the requirements for the Second Target Station and gave many good comments. This work was funded by Oak Ridge National Laboratory under the Laboratory Research and Development (LDRD) program.

References

[1] J. Wolters et al., in: Proceedings of the eighth International Topical Meeting on Nuclear Applications and Utilization of Accelerators, Pocatello, ID, August 2007.
[2] X.J. Jia, G.S. Bauer, W. He, Y.L. Sun, T.J. Liang, W. Yin, D. Zhao, Journal of Nuclear Materials, accepted for publication, doi:10.1016/j.jnucmat.2009.10.006.
[3] Eric J. Pitcher et al., in: Proceedings of the eighth International Topical Meeting on Nuclear Applications and Utilization of Accelerators, Pocatello, ID, August 2007.
[4] D. Pelowitz (Ed.), MCNPX User's Manual, Version 2.5.0, LA-CP-05-0369, Los Alamos National Laboratory, Los Alamos, April 2005.
[5] J. Mockus et al., Bayesian Heuristic Approach to Discrete and Global Optimization, Kluwer Academic Publishers, Boston/London/Dordrecht, 1996.
[6] SNS Second Target Station Conceptual Design Study, ORNL Report, Oak Ridge National Laboratory, Oak Ridge, September 2008.
[7] F.X. Gallmeier, Neutronics Analyses in Support of the SNS Rotating Target LDRD Project, STS03-31-TR0002-R00, Oak Ridge National Laboratory, May 2009.
[8] W. Lu, M.S. Wechsler, Y. Dai, Journal of Nuclear Materials 356 (2006) 280–286.
[9] F. Gallmeier et al., in: Proceedings of the eighth International Topical Meeting on Nuclear Applications and Utilization of Accelerators, Pocatello, ID, August 2007.
[10] E.B. Iverson, P.D. Ferguson, F.X. Gallmeier, B.D. Murphy, Journal of Neutron Research 11 (2003) 83–91.
[11] D. Nio, M. Ooi, N. Takenake, M. Furusake, M. Kawai, K. Mishima, Y. Kiyanagi, Journal of Nuclear Materials 343 (2005) 63–168.
[12] P.W. Dittus, L.M.K. Boelter, Univ. Calif. Pub. Eng. (2/13) (1930) 443–461 (Reprinted in Int. Comm. Heat Mass Transfer. 12 (1985) 3–22).